Table 4. The APC of childhood cancer mortality rates (girls)

Country	Period	APC	Trend 2	APC	Trend 3	APC	Trend 4	APC	AAPC	
	Years		Years		Years		Years		Last 10 observations	Last 5 observations
Total malignant tumors										
Japan	1970–1972	3.24	1972–1995	−3.21*	1995–1999	−6.46*	1999–2006	−0.57	−1.9*	−0.6
Canada	1970–2004	−3.42*							−3.4*	−3.4*
United States	1970–1977	−4.46*	1977–1995	−2.72*	1995–2005	−1.07*			−1.1*	−1.1*
Italy	1970–2003	−2.80*							−2.8*	−2.8*
UK	1970–2005	−2.73*							−2.7*	−2.7*
New Zealand	1970–2004	−2.57*							−2.6*	−2.6*
Leukemia										
Japan	1970–2006	−4.53*							−4.5*	−4.5*
Canada	1970–2004	−5.28*							−5.3*	−5.3*
United States	1970–1980	−6.09*	1980–2005	−3.14*					−3.1*	−3.1*
Italy	1970–2003	−4.33*							−4.3*	−4.3*
UK	1970–2005	−3.88*							−3.9*	−3.9*
New Zealand	1970–2004	−3.17*							−3.2*	−3.2*
Lymphomas										
Japan	1970–1991	−1.13	1991–2006	−11.85*					−11.8*	−11.8**
Canada	1970–2004	−4.55*							−4.6*	−4.6*
United States	1980–2005	−4.39*							−4.4*	−4.4*
Italy	1970–2003	−3.93*							−3.9*	−3.9*
UK	1970–2005	−4.56*							−4.6*	−4.6*
New Zealand	1970–2004	−0.35							−0.4	−0.4
Central nervous system tumors										
Japan	1980–2006	0.03							0.0	0.0
Canada	1980–2004	−1.50*							−1.5*	−1.5*
United States	1980–2005	−0.87*							−0.9*	−0.9*
Italy	1980–2003	−2.28*							−2.3*	−2.3*
UK	1980–2005	−1.68*							−1.7*	−1.7*
New Zealand	1980–2004	−2.32*							−2.3*	−2.3*
Malignant kidney tumors										
Japan	1976–2006	−3.98*							−4.0*	−4.0*
Canada	1970–2004	−2.90*							−2.9*	−2.9*
United States	1970–1991	−4.60*	1991–2005	0.16					0.2	0.2
Italy	1970–2003	−4.62*							−4.6*	−4.6*
UK	1970–2005	−3.49*							−3.5*	−3.5*
New Zealand	1970–2004	−2.91*							−2.9*	−2.9*
Malignant bone tumors										
Japan	1980–2006	−1.79*							−1.8*	−1.8*
Canada	1980–2004	−0.24							−0.2	−0.2
United States	1980–2005	−1.59*							−1.6*	−1.6*
Italy	1980–2003	−3.52*							−3.5*	−3.5*
UK	1980–2005	−2.22*							−2.2*	−2.2*
New Zealand	1980–2004	1.52							1.5	1.5

*$P < 0.05$.

APC is the annual per cent change; AAPC is average annual per cent change.

obtained in the current study. Research in Great Britain [9, 10], Italy [11] and Sweden [12] showed increased trends in childhood leukemia. A report from Britain indicated that small peaks in the incidence of ALL in 1976 and 1990 coincided with the years immediately following influenza epidemics [13]. Other explanations of the increased trend were characteristics of the environment, such as population mixing, although the etiology of cancer remains complicated and largely unknown.

The stable trend in mortality for childhood CNS tumor implied a modest increase trend in the incidence rate in Japan because of the survival improvement reported in childhood CNS tumors in developed countries in recent decades, while progress in therapy for brain tumors has not been as great as for leukemia. For CNS tumors, computed tomography, which was introduced in the 1970s, and magnetic resonance imaging, which has been used widely since the 1980s, has become

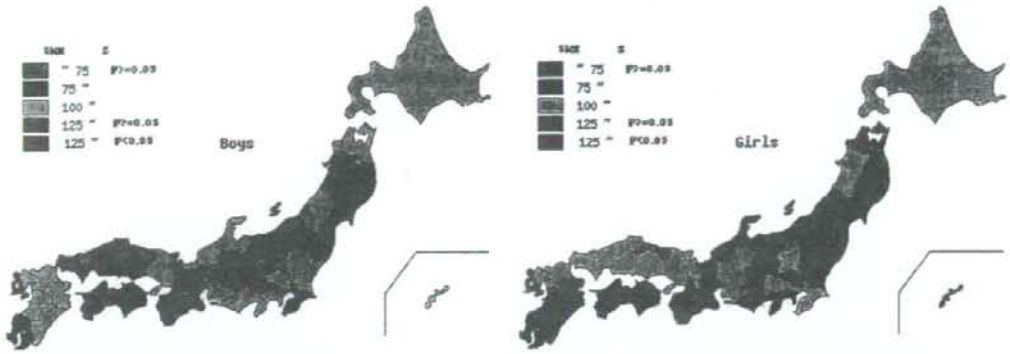

Figure 3. Standardized mortality ratios for childhood cancer in Japan, 2000–2006 by prefecture.

a standard tool for CNS tumor diagnosis and evaluation [14]. Furthermore, improvements in neurosurgical techniques have occurred during the past two decades, including stereotactic surgery, Cavitron Ultrasonic Surgical Aspirator and so on. Childhood cancer survival research from Osaka prefecture in Japan reported a slight increase in 5-year survival [1]. Incidence trends were not evaluated in this study. Data from the population-based cancer registry of Hokkaido prefecture in Japan indicated that the incidence of childhood brain tumors has been increasing, though the cause is unknown [15]. Other studies conducted in developed countries reported a significant increase in childhood CNS tumor incidence [10, 12, 16–21]. This has been explained by changes in detection and/or reports of childhood CNS tumors [22]. Because magnetic resonance imaging became ubiquitous at tertiary pediatric centers in the mid-1980s, it is likely to have increased the rate of detection; however, in the current study, the mortality rate of childhood CNS tumors in Japan was low and constant since the 1980s, and no significant increase in the number of deaths occurred in the middle of the 1980s to support the suggestion that the incidence increase was due to improved diagnostic techniques, if this increase really exists in Japan, and it seems unlikely to explain the long-term continued leveling off of mortality. The etiology of childhood CNS tumors remains largely unknown. Environmental factors are suggested to have a relationship with brain tumors. Further investigation in this field is needed to identify the incidence trends and reasonable explanations for these trends in Japan.

A previous childhood cancer mortality study in Japan presented data up to 1998. Furthermore, trend analysis was according to the correlation coefficient between the mortality rate and death year. Our analysis provides an updated mortality rate and reliable time trend analysis. In general, the mortality trends observed in other developed countries were compatible with Japan, although some differences were apparent. For example, a decrease in mortality during 0–14 years was observed in leukemia in the United States, Canada, Italy, New Zealand and Japan; however, the mortality rate from CNS tumors has decreased in the United States, Canada, UK and Italy in recent two decades. No evidence of decline appeared during 1980-2006 in Japan. For lymphoma, the decline occurred relatively late in Japan, compared with a significant decline without a leveling off period in the United States, Canada, Italy and UK. There is no simple explanation for these trend disparities. It is possible that the distribution of the histology pattern is markedly different among different countries, even in the same diagnostic group. The possible causes for these disparities in the childhood cancer death rate (e.g. late diagnosis, poor treatment quality, lack of health insurance and difficulty in accessing health care) need to be studied further.

A high mortality rate was observed in Kochi prefecture in boys and Tokushima and Kagoshima prefectures in girls. As mentioned above, the geographic disparity might be due to differences in cancer incidence and survival in different regions. Studies of the relationship between social class and childhood cancer have not been consistent. Research from Brazil suggested that higher decreases in the mortality rate were observed in more developed regions, possibly reflecting better health care [23]. We did not perform a similar ecologic study here, because of the small number of death, and we could not even calculate mortality by subtype by prefecture. Further detailed individual-level study is needed to identify a more reasonable explanation for the mortality disparities in childhood cancer.

A few points should be borne in mind when interpreting these findings. Some stable trends in the present study, such as mortality in lymphoma, and malignant bone tumors in New Zealand are more difficult to explain because of the small absolute number and substantial random variation. Other limitations included the wide time span and changes in diagnostic capabilities during the study period, and we were not able to collect any information on social status, employment of individuals and other genetic, environmental factors that would have allowed us to analysis etiological hypotheses.

Despite these limitations, when considering the absence of a national cancer registry system in Japan, estimates of incidence may have their own limitations (for example, they may be significantly influenced by errors in diagnosis and classification); evaluation of death may be an alternate effective method to identify more population-based point estimates of

doi:10.1093/annonc/mdn562 | 173

mortality from childhood cancer under these circumstances. Furthermore, the results presented here are based on 100% national coverage and provide an important baseline for monitoring the further progress against childhood cancer in Japan. Analysis of trends in national mortality rates over several decades may provide additional insight into the burden and impact of childhood cancer and suggest more targeted avenues for interventions that further delineate and ultimately reduce mortality from childhood cancer.

conclusions

The present study provides updated figures and trends in childhood cancer mortality in Japan and other developed countries. This will help to estimate care needs and to plan interventions and the quantity of appropriate childhood cancer treatment. Comprehensive efforts designed to identify risk factors for childhood cancer, promote early detection and reduce morbidity and mortality are warranted.

funding

Grant-in-Aid from the Ministry of Health, Labor, and Welfare of Japan (H19-GANRINSHO-IPPAN-012).

acknowledgements

Author contributions: LY designed and carried out analyses and drafted the paper; DQ prepared data and made the figure; JF, and NS edited the paper and commented on the interpretation of the result. All authors read and approved the final draft of the paper. Competing interests: The authors have no competing interests.

references

1. Ajiki W, Tsukuma H, Oshima A. Survival rates of childhood cancer patients in Osaka, Japan. Jpn J Clin Oncol 2004; 34: 50–54.
2. Cancer Facts and Figures 2007. American Cancer Society 2007.
3. Trends in childhood cancer mortality—United States, 1990–2004. Morb Mortal Wkly Rep 2007; 56: 1257–1261.
4. Steliarova-Foucher E, Stiller C, Kaatsch P et al. Geographical patterns and time trends of cancer incidence and survival among children and adolescents in Europe since the 1970s (the ACCISproject): an epidemiological study. Lancet 2004; 364: 2097–2105.
5. Zuccolo L, Pastore G, Maule M et al. Time trends of childhood cancer mortality rates: a report from the Childhood Cancer Registry of Piedmont, Italy, 1971–1998. Pediatr Blood Cancer 2004; 43: 788–791.
6. Kim HJ, Fay MP, Feuer EJ, Midthune DN. Permutation tests for joinpoint regression with applications to cancer rates. Stat Med 2000; 19: 335–351.
7. National Cancer Institute. http://srab.cancer.gov/joinpoint/aapc.html (1 July 2008, date last accessed).
8. Coebergh JW, Reedijk AM, de Vries E et al. Leukaemia incidence and survival in children and adolescents in Europe during 1978–1997. Report from the Automated Childhood Cancer Information System project. Eur J Cancer 2006; 42: 2019–2036.
9. Feltbower RG, Moorman AV, Dovey G et al. Incidence of childhood acute lymphoblastic leukaemia in Yorkshire, UK. Lancet 2001; 358: 385–387.
10. McNally RJ, Kelsey AM, Cairns DP et al. Temporal increases in the incidence of childhood solid tumors seen in Northwest England (1954–1998) are likely to be real. Cancer 2001; 92: 1967–1976.
11. Maule MM, Zuccolo L, Magnani C et al. Bayesian methods for early detection of changes in childhood cancer incidence: trends for acute lymphoblastic leukaemia are consistent with an infectious aetiology. Eur J Cancer 2006; 42: 78–83.
12. Dreifaldt AC, Carlberg M, Hardell L. Increasing incidence rates of childhood malignant diseases in Sweden during the period 1960–1998. Eur J Cancer 2004; 40: 1351–1360.
13. Kroll ME, Draper GJ, Stiller CA, Murphy MF. Childhood leukemia incidence in Britain, 1974–2000: time trends and possible relation to influenza epidemics. J Natl Cancer Inst 2006; 98: 417–420.
14. Prados MD, Berger MS, Wilson CB. Primary central nervous system tumors: advances in knowledge and treatment. CA Cancer J Clin 1998; 48: 331–360, 321.
15. Nishi M, Miyake H, Takeda T, Hatae Y. Epidemiology of childhood brain tumors in Japan. Int J Oncol 1999; 15: 721–725.
16. Hjalmars U, Kulldorff M, Wahlqvist Y, Lannering B. Increased incidence rates but no space-time clustering of childhood astrocytoma in Sweden, 1973–1992: a population-based study of pediatric brain tumors. Cancer 1999; 85: 2077–2090.
17. Bunin GR, Feuer EJ, Witman PA, Meadows AT. Increasing incidence of childhood cancer: report of 20 years experience from the greater Delaware Valley Pediatric Tumor Registry. Paediatr Perinat Epidemiol 1996; 10: 319–338.
18. Draper GJ, Kroll ME, Stiller CA. Childhood cancer. Cancer Surv 1994; 19–20: 493–517.
19. Dalmasso P, Pastore G, Zuccolo L et al. Temporal trends in the incidence of childhood leukemia, lymphomas and solid tumors in north-west Italy, 1967–2001. A report of the Childhood Cancer Registry of Piedmont. Haematologica 2005; 90: 1197–1204.
20. Hauser P, Jakab Z, Lang O et al. High incidence of brain tumors of childhood in Hungary between 1989 and 2001. Med Pediatr Oncol 2003; 41: 590–591.
21. Crocetti E, Bernini G, Tamburini A et al. Incidence and survival cancer trends in children and adolescents in the Provinces of Florence and Prato (Central Italy), 1985–1997. Tumori 2002; 88: 461–466.
22. Smith MA, Freidlin B, Ries LA, Simon R. Trends in reported incidence of primary malignant brain tumors in children in the United States. J Natl Cancer Inst 1998; 90: 1269–1277.
23. Ribeiro KB, Lopes LF, de Camargo B. Trends in childhood leukemia mortality in Brazil and correlation with social inequalities. Cancer 2007; 110: 1823–1831.

CLONING AND STEM CELLS
Volume 10, Number 3, 2008

DOI: 10.1089/clo.2008.0024

Transgenic-Cloned Pigs Systemically Expressing Red Fluorescent Protein, Kusabira-Orange

Hitomi Matsunari,[1] Masafumi Onodera,[2] Norihiro Tada,[3] Hideki Mochizuki,[4] Satoshi Karasawa,[5,6,7] Erika Haruyama,[1] Naoki Nakayama,[1] Hitoshi Saito,[1] Satoshi Ueno,[1] Mayuko Kurome,[1] Atsushi Miyawaki,[5] and Hiroshi Nagashima[1]

Abstract

Genetically engineered pigs with cell markers such as fluorescent proteins are highly useful in lines of research that include the tracking of transplanted cells or tissues. In this study, we produced transgenic-cloned pigs carrying a gene for the newly developed red fluorescent protein, humanized Kusabira-Orange (huKO), which was cloned from the coral stone *Fungia concinna*. The nuclear transfer embryos, reconstructed with fetal fibroblast cells that had been transduced with huKO cDNA using retroviral vector DΔNsap, developed efficiently *in vitro* into blastocysts (28.0%, 37/132). Nearly all (94.6%, 35/37) of the cloned blastocysts derived from the transduced cells exhibited clear huKO gene expression. A total of 429 nuclear transfer embryos were transferred to four recipients, all of which became pregnant and gave birth to 18 transgenic-cloned offspring in total. All of the pigs highly expressed huKO fluorescence in all of the 23 organs and tissues analyzed, including the brain, eyes, intestinal and reproductive organs, skeletal muscle, bone, skin, and hoof. Furthermore, such expression was also confirmed by histological analyses of various tissues such as pancreatic islets, renal corpuscles, neuronal and glial cells, the retina, chondrocytes, and hematopoietic cells. These data demonstrate that transgenic-cloned pigs exhibiting systemic red fluorescence expression can be efficiently produced by nuclear transfer of somatic cells retrovirally transduced with huKO gene.

Introduction

PIGS HAVE BEEN INCREASINGLY USED as large animal models in biomedical research (Lunney, 2007; Petters, 1994; Prather et al., 2003). For example, as they are comparatively larger than rodents, various surgical procedures that have been performed on humans can be applied to the pig (for review, see Lunney, 2007). The anatomical and physiological similarities of pigs and humans also offer a potential solution to the problem that murine studies cannot necessarily be extrapolated to humans (Lunney, 2007; Petters, 1994; Prather et al., 2003). Thus, genetically engineered pigs produced as human disease models are expected to cover the shortcomings of rodent models (Petters et al., 1997; Rogers et al., 2008). Furthermore, in order to render stem and progenitor cell-based therapies more feasible for the treatment of various intractable disorders, research must be conducted not only in rodent animal models, but also in large animal models such as pigs (Lunney, 2007; Matsumoto et al., 2007).

Under these circumstances, genetically engineered animals with cell markers such as fluorescent proteins are highly useful in lines of research, which include the tracking of transplanted cells or tissues (Hadjantonakis and Nagy, 2001; Murakami and Kobayashi, 2005; Okabe et al., 1997; Yin et al., 2007). Transgenic pigs expressing enhanced green fluorescent protein (EGFP) have been produced by various re-

[1]Laboratory of Developmental Engineering, Department of Life Science, School of Agriculture, Meiji University, Kawasaki 214-8571, Kanagawa, Japan.
[2]Advanced Biomedical Applications, Graduate School of Comprehensive Human Sciences, University of Tsukuba, Tsukuba 305-8575, Ibaraki, Japan.
[3]Division of Genome Research, Atopy (Allergy) Research Center, Graduate School of Medicine, Juntendo University, Bunkyo-ku 113-8421, Tokyo, Japan.
[4]Department of Neurology, Juntendo University, Bunkyo-ku 113-8421, Tokyo, Japan.
[5]Laboratory for Cell Function and Dynamics, Advanced Technology Development Group, Brain Science Institute, RIKEN, Wako 351-0198, Saitama, Japan.
[6]Amalgaam Co., Ltd., Itabashi-ku 173-0004, Tokyo, Japan.
[7]Medical & Biological Laboratories Co., Ltd., Nagoya 460-0018, Aichi, Japan.

search groups (Cabot et al., 2001; Hofmann et al., 2003; Hyun et al., 2003; Lai et al., 2002; Naruse et al., 2005; Park et al., 2002; Watanabe et al., 2005; Webster et al., 2005; Whitelaw et al., 2004; Yong et al., 2006). On the other hand, rodents expressing not only EGFP but also various other markers have been produced, making rodents a useful model for a wide range of research (Luche et al., 2007; Murakami and Kobayashi, 2005; Sato et al., 2003; Vintersten et al., 2004). Indeed, red fluorescent protein (RFP) variants with longer excitation/emission wavelengths than EGFP offer benefits for genetically and spectrally distinct imaging of multiple cell populations in complex tissues (Long et al., 2005). Webster et al. (2005) reported the production of transgenic pigs that simultaneously express DsRed (DsRed2; Long et al., 2005) in addition to EGFP. However, the effect of using DsRed, which is highly cytotoxic (Long et al., 2005), in transgenic pigs has not been clarified.

In the present study, we produced transgenic-cloned pigs carrying the huKO gene (Karasawa et al., 2004), a newly developed RFP. Kusabira-Orange, which was cloned from the coral stone *Fungia concinna* ("Kusabira-Ishi" in Japanese), yields an orange-red fluorescence in dimeric form with a 558/583 nm excitation/emission maxima, respectively (Karasawa et al., 2004). We performed somatic cell nuclear transfer (SCNT) using fetal fibroblast cells that were transduced with the huKO gene by a retroviral vector. The production efficiency, embryonic development, and *in vitro* fluorescence expression of the cloned embryos were investigated. We were able to successfully produce transgenic-cloned pigs with a high efficiency by transfer of SCNT embryos. In addition, systemic red fluorescence expression was confirmed in all cloned pigs produced in the present study.

Materials and Methods

Animal care and chemicals

All of the animal experiments in this study were approved by the Institutional Animal Care and Used Committee of Meiji University (IAUCU-05-003). Chemicals were purchased from Sigma Chemical Co. (St. Louis, MO) unless otherwise indicated.

Construction of DΔNsap expressing huKO gene

The retroviral vector DΔNsap was constructed from previously reported vector, GCDsap (Hamanaka et al., 2007). Briefly, the binding site for Ying-Yang1 (YY1) transcription factor (Wahlers et al., 2002), referred to as the negative control region (NCR), in the PCC4 cell-passaged myeloproliferative sarcoma virus (PCMV)-derived LTR of GCDsap (Hamanaka et al., 2007) was abolished by site-directed mutagenesis using a PCR technique (Fig. 1A). *Nco*I–*Not*I fragments of the huKO cDNA were inserted into the *Nco*I–*Not*I digested vector to generate DΔNsaphuKO (Fig. 1A). The vector was converted to the corresponding retroviruses packaged in the vesicular stomatitis virus G protein (VSV-G) envelope by transduction into 293gpg cells, as described elsewhere (Suzuki et al., 2002a). The virus titer of DΔNsaphuKO was approximately 2.0×10^7 infectious units (I.U.)/mL, as assessed in Jurkat cells. No replication-competent retrovirus was detected.

Transduction of huKO into nuclear donor cells

In this study, the huKO cDNA synthesized by humanizing the original amino acid sequence of Kusabira-Orange gene (Karasawa et al., 2004) was used as a fluorescent marker.

A primary culture of fetal fibroblasts was established from a day 30 porcine female fetus (Crossbred: Large White/Landrace × Duroc) following the standard procedure (Freshney, 2005; Kurome et al., 2003). Established cells were cultured in Dulbecco Modified Eagle medium (DMEM; D6546) supplemented with 15% fetal bovine serum (FBS; Code No. 12303C, JRH Biosciences, Lexena, KS) and cryopreserved after two to six passages. For transduction, the frozen–thawed cells suspended in 5 mL Knockout DMEM (Invitrogen Corp., Carlsbad, CA) supplemented with 10% (v/v) FBS (ES Cell Qualified FBS, Code No. 16141-079, Invitrogen) at the concentration of 1×10^6/mL were transferred into a gelatin-coated six-well dish and transduced with the DΔNsaphuKO by adding 30 μL (multiplicity of infection = 0.12) of the virus supernatant to the culture. At 48 h after transduction, the cells were washed with PBS twice and transferred into a new six-well dish containing the same medium. The transduced cells were cryopreserved after 15–16 passages.

In vitro *maturation of recipient oocytes*

Porcine ovaries were collected at a local abattoir and transported to the laboratory in PBS containing 75 μg/mL potassium penicillin G, 50 μg/mL streptomycin sulfate, 2.5 μg/mL amphotericin B, and 0.1% (v/v) polyvinyl alcohol (PVA). Cumulus–oocyte complexes were collected from the ovarian antral follicles (3.0 to 6.0 mm in diameter) by aspirating with a 10-mL syringe and 20 G hypodermic needle, and those with at least three layers of compacted cumulus cells were selected and cultured in NCSU23 medium (Petters and Wells, 1993) supplemented with 0.6 mM cysteine, 10 ng/mL epidermal growth factor, 10% (v/v) porcine follicular fluid, 75 μg/mL potassium penicillin G, 50 μg/mL streptomycin sulfate, 10 IU/mL eCG (ASKA Pharmaceutical. Co., Tokyo, Japan), and 10 IU/mL hCG (ASKA Pharmaceutical) at 38.5°C in a humidified atmosphere of 5% CO_2 in air for 22 h. Then, oocytes were cultured for an additional 22 h without eCG and hCG (Funahashi and Day, 1993). *In vitro* matured (IVM) oocytes with expanded cumulus cells were treated with 1 mg/mL of hyaluronidase dissolved in Tyrode lactose medium containing 10 mM HEPES and 0.3% (w/v) polyvinylpyrrolidone (HEPES-TL-PVP), and separated from the cumulus cells by gentle pipetting. Oocytes with an evenly granulated ooplasm and an extruded first polar body were selected for the subsequent experiments.

Nuclear transfer of huKO-transduced fibroblasts into IVM oocytes

Somatic cell nuclear transfer of porcine fetal fibroblasts into enucleated oocytes was performed as described elsewhere (Kurome et al., 2003; Tomii et al., 2005; Yin et al., 2002). Oocytes were cultured in NCSU23 medium supplemented with 0.1 μg/mL demecolcine, 0.5 M sucrose (Nacalai Tesque, Inc., Kyoto, Japan) and 4 mg/mL BSA (Fruction V, A-4919) for 0.5 to 1 h, and enucleated by aspirating the first polar body and adjacent cytoplasm using a beveled pipette (30 μm

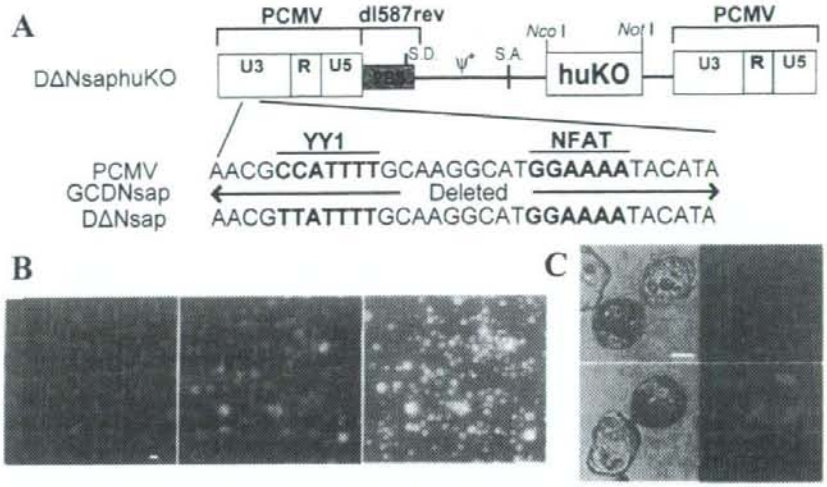

FIG. 1. Retroviral vector construct, transduced nuclear donor cells and cloned blastocysts reconstructed with transduced cells. (**A**) Structure of the retroviral vector DΔNsaphuKO. DΔNsap has the PCMV derived LTR in which the binding site for YY1 (CCATTTT) was abolished by site-directed mutagenesis with PCR while the NFAT binding site (GGAAAA) is still functional. In contrast, GCDNsap from which DΔNsap has been generated has the PCMV-derived LTR that lacks both of the binding sites for YY1 and NFAT. The *Nco*I–*Not*I fragments containing huKO cDNA were cloned into the corresponding site of the vector. A dark box represents the primer-binding site (PBS) derived from the dl587rev. Abbreviations present in the vector are labeled as follows; PCMV: PCC4-cell passaged myeloproliferative sarcoma virus, Ψ^+: packaging signal, S.D and S.A: splice donor and acceptor sequences. (**B**) Porcine fetal fibroblast cells expressing huKO after retroviral transduction (left panel), and the nuclear donor cells (middle panel) used for cloning the pigs. A merged picture (right panel) shows that over 80% of the donor cells were positive for huKO expression. Scale bar = 20 μm. (**C**) Cloned blastocysts (upper and lower left panels) were produced by nuclear transfer of the transduced cells. Note that the huKO expression level of these embryos varies (upper and lower right panels). Scale bar = 50 μm.

in diameter) in HEPES-TL-PVP containing 0.1 μg/mL demecolcine, 5 μg/mL cytochalasin B (CB), and 10% FBS. When a protrusion was observed on the surface of an oocyte, it was removed along with the polar body. Enucleation was confirmed by staining the cytoplasts with 5 μg/mL bisbenzimide (Hoechst 33324).

Porcine fetal fibroblasts transduced with the huKO cDNA and control, nontransduced cells, which had been respectively cryopreserved after 15–16 or 5–6 passages, were used as nuclear donors. After thawing, the cell cycles of the donor cells were synchronized by serum starvation (0.5% ES Cell Qualified FBS for transduced cells and 0.5% FBS for control cells) for 48 h. A single donor cell was inserted into the perivitelline space of an enucleated oocyte. The donor cell–oocyte complexes were suspended in mannitol solution (280 mM, pH 7.2) containing 0.15 mM $MgSO_4$, 0.01% (w/v) PVA and 0.5 mM HEPES and held between two electrode needles. Membrane fusion was induced with a somatic hybridizer (SSH-1; Shimadzu, Koyto, Japan) by applying a single direct current (DC) pulse (187 to 200 V/mm, 20 μsec $\times$1) and a pre- and postpulse alternating current (AC) field of 5 V, 1 MHz for 5 sec, respectively. The reconstructed embryos were cul-

FIG. 2. Transgenic-cloned fetus and pigs produced by SCNT of huKO fetal fibroblast cells transduced with huKO gene. A day-47 fetus (**A**) with systemic fluorescence expression (scale bar = 1 cm). Newborn offspring (**B**) and a fully matured gilt (**C**; O18-3, 17-month-old).

tured in the NCSU23 medium with 4 mg/mL BSA for 1 to 1.5 h followed by electrical activation (DC 150 V/mm, 100 μsec ×1) and subsequent treatment with 5 μg/mL CB for 3 h to suppress extrusion of the pseudosecond polar body.

Cleavage, blastocyst formation, and expression of huKO gene in the early developmental stage of the cloned embryos were monitored during culture for 7 days. *In vitro* culture of the embryos was performed in 20 μL droplets of modified NCSU23 (Nagashima et al., 2007). On day 7 embryos were examined under fluorescent microscopy (TE-300, Nikon, Tokyo, Japan), and the cell number of blastocysts was also counted after fixation and staining.

Transfer of cloned embryos into recipient pigs

Crossbred (Large White/Landrace × Duroc) prepubertal gilts weighing from 100 to 105 kg were used as recipients of the embryos. For the induction of estrus, gilts were intramuscularly injected with 1000 IU of eCG (ASKA Pharmaceutical, Tokyo, Japan) followed by 1500 IU of hCG (Kawasaki Mitaka Pharmaceutical. Co., Kawasaki, Japan) 72 h later. Having been cultured in the Porcine Zygote Medium-5 (PZM-5; Functional Peptide Inc., Yamagata, Japan) for 1 to 2 days, embryos with a normal morphological appearance and at the one-cell stage on days 1 and two to eight-cell stage on day 2, were selected and transferred into oviducts of the recipient gilts that had received hCG injection 48 h previously.

Analysis of huKO expression in the transgenic-cloned pigs

Transgenic-cloned offspring were autopsied to collect small snips of 23 organs and tissues in total, including the brain, heart, lung, stomach, intestine, liver, pancreas, spleen, kidney, bladder, ovary, uterus, skin, subcutaneous fat, skeletal muscle, bone (rib), cartilage, synovium, salivary gland, oral mucosa, tongue, eye, and hoof. These tissues were observed under MVX10 fluorescence stereomicroscopy (Olympus, Tokyo, Japan; excitation wavelength: 530–555 nm, absorption filter: 570–625 nm) to examine huKO expression. Paraffin-embedded sections of those organs and tissues were also observed under fluorescence microscopy (Olympus BX52, excitation wavelength: 520–550 nm, absorption filter: 580 nm).

For immunohistochemistry of the brain, cryosections were stained with antidoublecortin (DCX) antibody (polyclonal goat IgG, Santa Cruz Biotechnology Inc., Santa Cruz, CA), antimicrotubule-associated protein (MAP2) antibody (monoclonal mouse IgG, Upstate Co., Charlottesville, VA), anti-ionized calcium binding adaptor protein (Iba1) antibody (polyclonal rabbit IgG, Wako, Osaka, Japan), and antiglial fibrillary acidic protein (GFAP) antibody (polyclonal rabbit IgG; a generous gift from Dr. Haruhiko Akiyama, Psychiatric Research Institute of Tokyo, Tokyo, Japan), followed by staining with FITC-labeled secondary antibody (Hayakawa et al., 2007; Yamada et al., 2004). Images of sections were obtained using an LSM-510 laser-scanning microscope (Carl Zeiss, Oberkochen, Germany).

Expression of huKO gene was analyzed in blood cells and subcutaneous fat tissue of a growing pig (O18-3). Peripheral blood was collected from a 4-month-old transgenic-cloned pig (O18-3). Each hematopoietic lineage grouped by both forward scatter (FSC) and side scatter (SSC) values was analyzed for huKO expression using FACS calibur (Becton Dickinson, San Jose, CA). A small snip of subcutaneous fat tissue collected from the same pig at 7 and 17 months after birth was observed under fluorescence microscopy (BZ-8000, Keyence, Osaka, Japan; excitation wavelength: 525–540 nm, absorption filter: 605–655 nm).

Southern blot analysis

High molecular-weight DNA was isolated from the skin or kidney of the cloned offspring and a control wild-type piglet. Ten micrograms of genomic DNA was digested with *Bam*HI overnight, separated in 1% agarose gel, transferred to a nylon membrane (GE Healthcare UK Ltd., Buckinghamshire, England), and hybridized to [α-^{32}P] CTP labeled huKO cDNA. The restriction enzyme *Bam*HI cuts the vector at one site, and therefore the number of fragments hybridized with the probe is considered to be the number of provirus copies integrated into the host genomes.

Statistical analysis

For proportional data, differences between groups were analyzed using the χ^2 test. For blastocyst cell number data, differences between groups were determined by Student's *t*-test. The level of significance was set at $p < 0.05$.

Results

Production of cloned embryos by nuclear transfer of huKO expressing cells

When the fibroblasts were exposed to the concentrated virus supernatant, approximately 80% of the cells highly ex-

TABLE 1. *IN VITRO* DEVELOPMENT AND HUKO EXPRESSION OF THE CLONED EMBRYOS RECONSTRUCTED WITH RETROVIRALLY TRANSDUCED CELLS

		Embryonic development (%)			
Donor cells	*Fusion rate*	*Cleaved*	*Blastocysts*	*Cell number in blastocysts (Mean ± SEM)*	*huKO expressing blastocysts (%)*
huKO-PFF	132/151 (87.4)	78/132 (59.1)	37/132 (28.0)[a]	48.6 ± 4.8	35/37 (94.6)
PFF	134/147 (91.2)	86/134 (64.2)	20/134 (14.9)[a]	42.3 ± 4.9	0/20 (0)

huKO-PFF, porcine fetal fibroblast cells transduced with DΔNsaphuKO; PFF, nontransduced fetal fibroblast cells.
[a] $p < 0.05$.

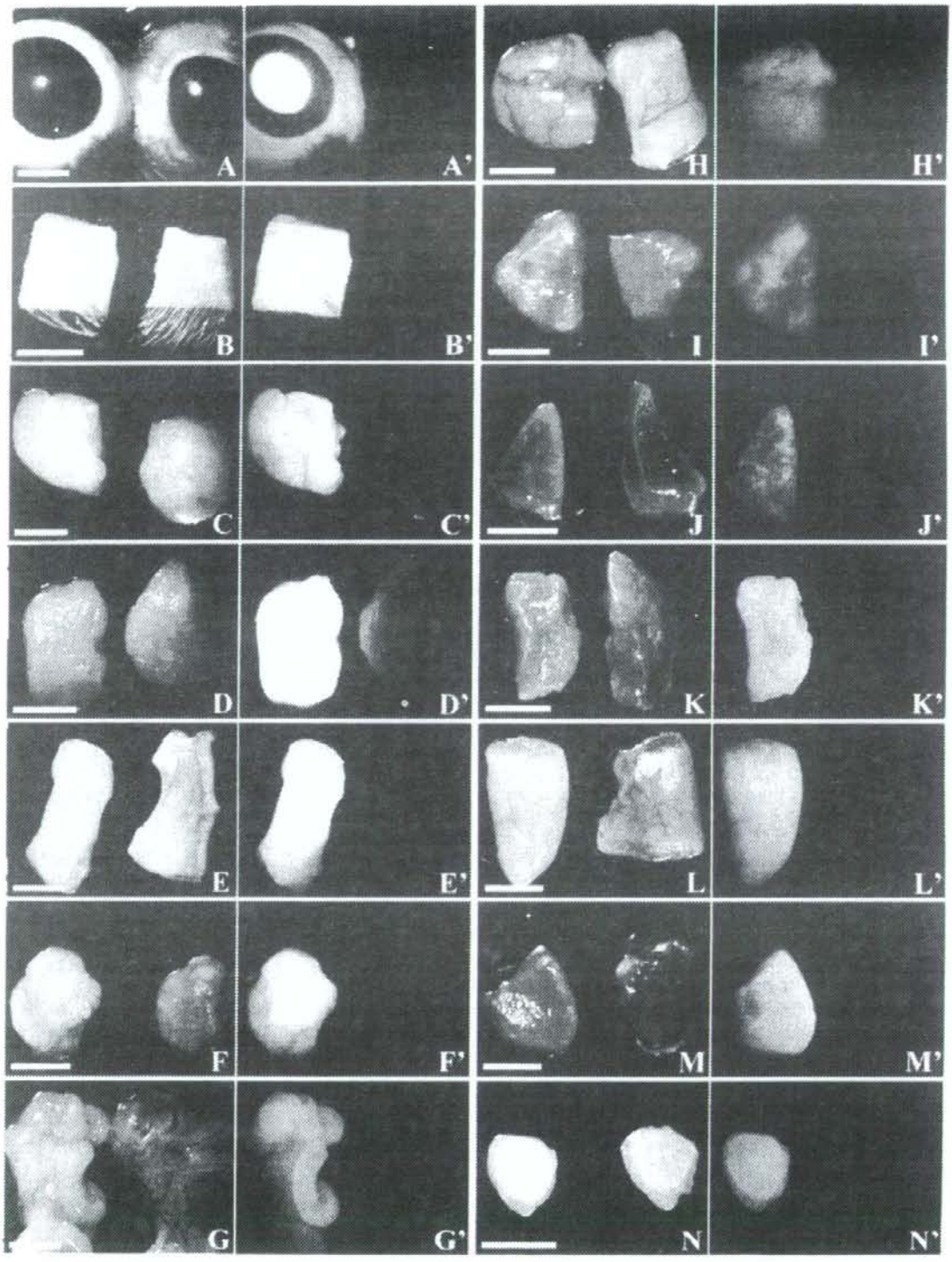

FIG. 3. Systemic expression of huKO in transgenic-cloned pigs. (**A–N**) Bright-field stereomicroscopic images of tissues from a transgenic-cloned offspring (left) and nontransgenic control (right). (**A'–N'**) Fluorescence stereomicroscopic images demonstrate that tissues from the transgenic-cloned pig (left) exhibit distinctive fluorescence, while none of the control tissues (right) has background autofluorescence. eye (**A**,**A'**); skin (**B**,**B'**); salivary gland (**C**,**C'**); skeletal muscle (**D**,**D'**); stomach (**E**,**E'**); pancreas (**F**,**F'**); reproductive tract and ovary (**G**,**G'**); brain (**H**,**H'**); lung (**I**,**I'**); liver (**J**,**J'**); heart (**K**,**K'**); intestine (**L**,**L'**); kidney (**M**,**M'**); bone[rib] (**N**,**N'**). Scale bar = 5 mm.

pressed huKO (Fig. 1B), and such expression was maintained in porcine nuclear transfer embryos reconstructed with the transduced fibroblasts (Fig. 1C). As shown in Table 1, nearly all (94.6%, 35/37) of the cloned blastocysts derived from the transduced cells clearly exhibited evident huKO expression, although the level of fluorescence varied among the embryos (Fig. 1C). Efficiency of cell fusion and early cleavage of the cloned embryos using transduced cells as nuclear donors was comparable to that with control nontransduced fibroblasts (Table 1). Furthermore, the rate of *in vitro* blastocyst formation of the cloned embryos reconstructed with transduced cells was rather higher than that of control embryos derived from nontransduced cells (Table 1).

Development of transgenic-cloned pigs transduced with huKO gene

Having determined that the expression of huKO gene had very few, if any, detrimental effects on the development of porcine embryos per se, the embryos were transferred into the oviducts of five estrus-synchronized recipient gilts. Three fetuses (day 47) were obtained from one recipient into which 76 cloned embryos had been transferred (Fig. 2A). When 429 of the nuclear transfer embryos in total had been transferred to four recipients, all of them became pregnant and gave birth to 18 offspring (Fig. 2B), including four cases of stillbirth. The average body weight and length of these offspring were 1068.2 ± 77.4 g and 22.7 ± 0.7 cm, respectively (mean ± SEM). The production efficiency of the transgenic-cloned offspring and fetuses from the retrovirally transduced cells was 4.2%.

Expression of huKO gene in the entire body of the cloned pigs

Fluorescence stereomicroscopic examination revealed that both the fetuses and offspring highly expressed huKO ubiquitously throughout their entire bodies (Fig. 3). Furthermore, histological analysis of 23 various organs and tissues confirmed the high expression of huKO, although the intensity of expression varied among these organs (Fig. 4). Expression of huKO fluorescence at the red wavelength could be clearly detected in the liver without any interference from autofluorescence (Fig. 3J, J', Fig. 4J, J'). Interestingly, the pancreatic islets (Fig. 4I, I') and renal corpuscles (Fig. 4K, K') exhibited markedly prominent red fluorescence compared to the surrounding tissues. Prominent expression of huKO was also detected in other tissues, such as the crystalline lens (Fig. 3A, A', Fig. 4 A, A') and the acinus of the submandibular gland (Fig. 3C, C', Fig. 4C, C').

The expression of huKO in neurons and glial cells was observed in immunostaining with neuron- or glia-specific antibodies such as DCX and MAP2 or Iba1 and GFAP, respectively (Fig. 5).

Analysis of peripheral blood cells collected from a 4-month-old transgenic-cloned pig (O18-3) by FACS calibur revealed that huKO was expressed in hematopoietic cells, including granulocytes, monocytes, lymphocytes, and platelets, although the expression of huKO in red blood cells (RBC) was much lower than that of other lineages (Fig. 6).

As shown in Fig. 7, fluorescence expression level of subcutaneous fat tissue observed at 7 months after birth (A, A') was maintained even at 17 months (B, B').

Multiple copies of the provirus in cloned pigs

To determine the number of copies of the provirus integrated into the chromosomes of cloned pigs, high molecular-weight DNA was obtained from 12 cloned pigs and hybridized with the huKO cDNA as a probe following digestion with the restriction enzyme *Bam*HI, which cuts the vector at one site. As shown in Figure 8A, Southern blot analysis revealed that each pig had multiple copies of the provirus ranging from 2 to 17, suggesting that cloned pigs developed by nuclear transfer stably maintained the transgene in their chromosomes through ontogenesis and resulted in high expression of huKO in the whole body.

All of the four transgenic pigs showing lower fluorescence expression level were revealed to have fewer copy numbers (2–6) of the provirus (Fig. 8BC, B'C'). In contrast, six other transgenic pigs with higher huKO expression level had higher (≥9) copies of provirus (Fig. 8D–G, D'–G'), except for one with two copies of the transgene.

Discussion

The SCNT approach described here, combined with the retrovirus-mediated gene transfer method, allowed stable expression of the transgene in cloned pigs that were developed from embryos reconstructed with fetal fibroblasts transduced with the huKO cDNA. To the best of our knowledge, this is the first report on the production of transgenic-cloned pigs expressing Kusabira-Orange.

The production efficiency (4.2%) of the transgenic-cloned offspring in this study was comparable to that observed in nuclear transfer experiments using nontransgenic donor cells in previous reports by both our group and other researchers (Kurome et al., 2006; Tomii et al., 2005; Walker et al., 2002). The high clone production efficiency observed was likely ascribable to the preparation of high-quality nuclear donor cells. Drug selection of the transfected nuclear donor cells for a relatively long period of time has been reported to induce chromosomal aberrance (Forsberg et al., 2002; Fujimura et al., 2008; Iguma et al., 2005; Zakhartchenko et al., 2001), resulting in a significant reduction of the birth rate of clones. In contrast, we were able to use retrovirally transduced fetal fibroblasts as the nuclear donor cells without any selection procedures, because more than 80% of the cells had highly expressed huKO after one round of transduction. Retroviral integration into donor cells per se was also unlikely to be toxic, as demonstrated by the fact that 82% (data

FIG. 4. Histological analysis of various tissues from the transgenic-cloned pigs with systemic huKO expression. HE stained (**A–P**) and fluorescence microscopy (**A'–P'**) of paraffin-embedded serial sections of huKO transgenic-cloned piglets. eye (**A,A'**); tongue (**B,B'**); salivary gland (**C,C'**); intestine (**D,D'**); spleen (**E,E'**); bladder (**F,F'**); uterus (**G,G'**); hoof (**H,H'**); pancreas (**I,I'**); liver (**J,J'**); kidney (**K,K'**); ovary (**L,L'**); subcutaneous fat (**M,M'**); cartilage (**N,N'**); synovium (**O,O'**); hard palate (**P,P'**). Note that the islets of Langerhans (**I,I'**) and renal corpuscles (**K,K'**) indicated by the arrows display prominent red fluorescence compared to the surrounding tissues. Scale bar = 1 cm (**A**); 500 μm (**B–H**) and 100 μm (**I–P**).

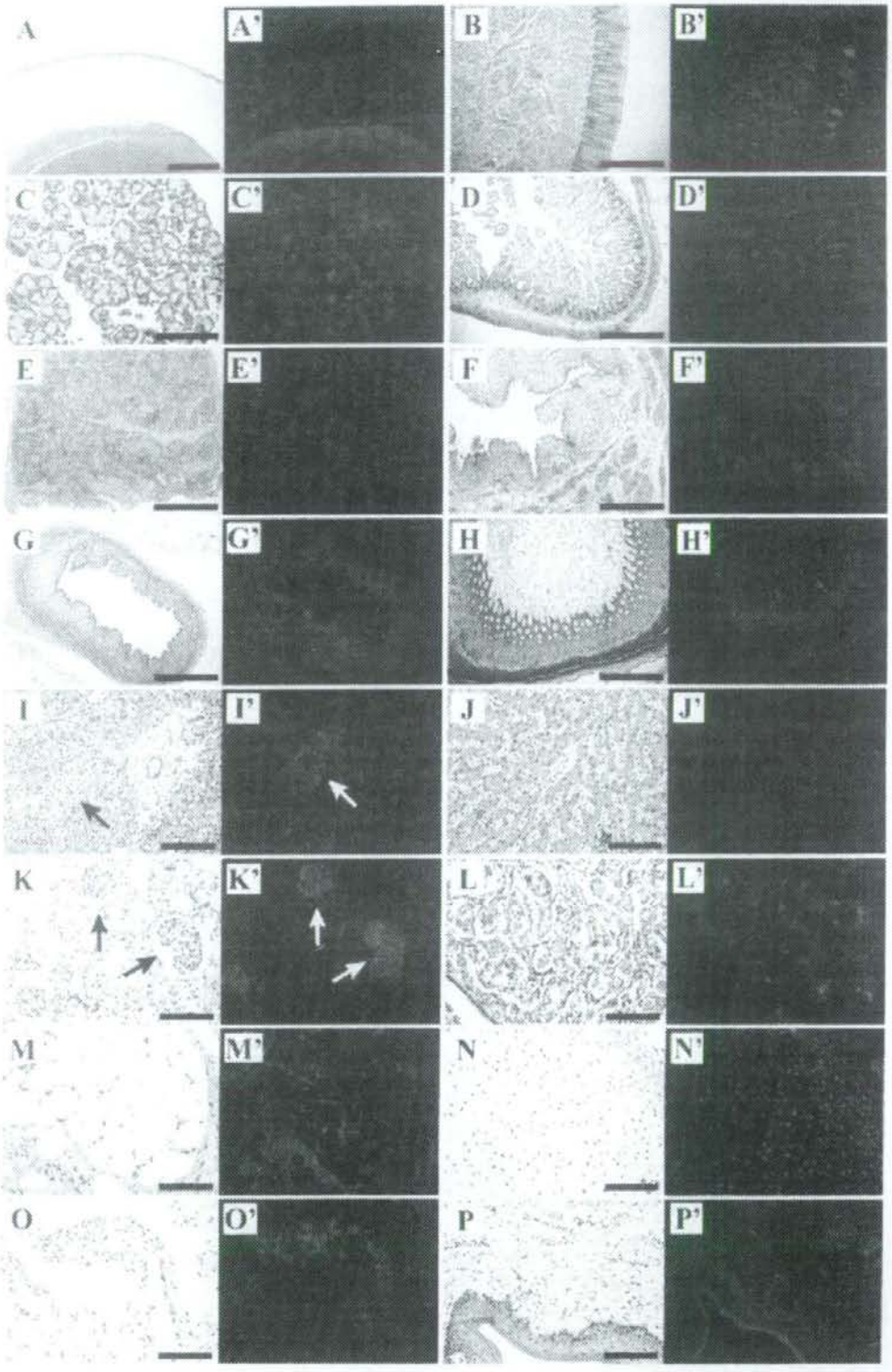

FIG. 4.

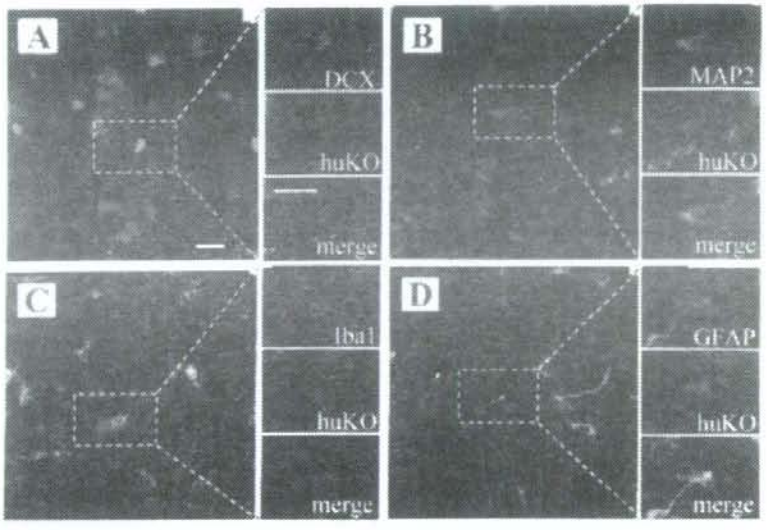

FIG. 5. Immunofluorescent staining of neural cells from huKO transgenic-cloned pigs. To examine huKO expression in neuronal and glial cells, brain tissue sections were examined by immunofluorescent staining and fluorescence microscopy. The boxed insets show that huKO expression was colocalized with DCX (**A**), MAP2 (**B**), Iba1 (**C**), and GFAP (**D**), which are markers for neuron progenitors, mature neurons, microglia, and astrocytes, respectively. Scale bar = 20 μm.

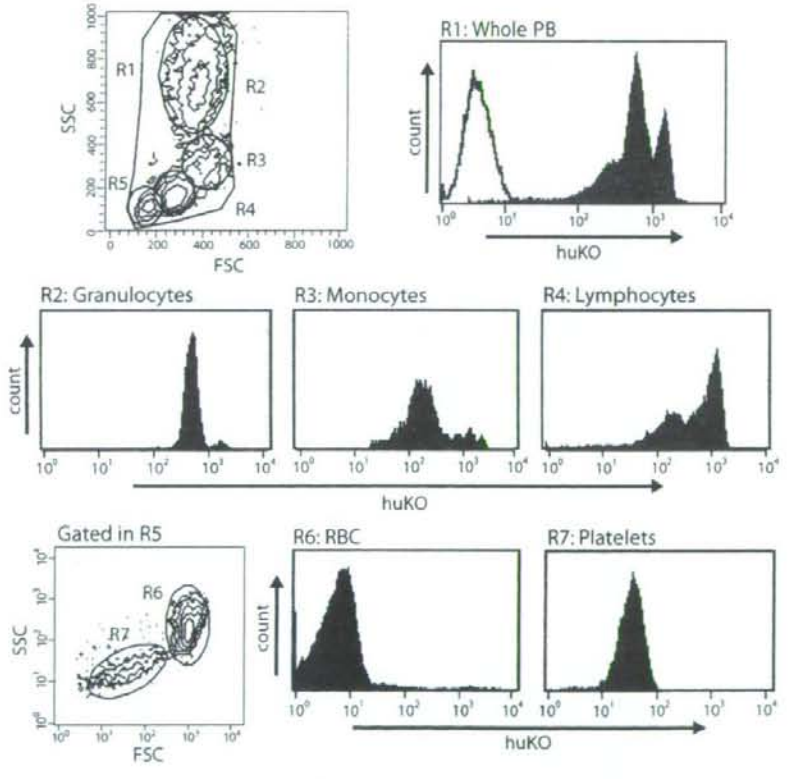

FIG. 6. Expression of huKO in peripheral blood of a transgenic-cloned pig. Peripheral blood was collected from a 4-month-old transgenic-cloned pig (O18-3) and analyzed with FACS calibur. The population of each lineage was classified by both forward scatter (FSC) and side scatter (SSC) values of the flow cytometry. The R6 (RBC) and R7 (platelet) were gated from the R5. Each hematopoietic lineage (R2: granulocytes, R3: monocytes, R4: lymphocytes, R6: RBC, and R7: platelets) in the peripheral blood of the cloned pigs was analyzed in terms of huKO expression.

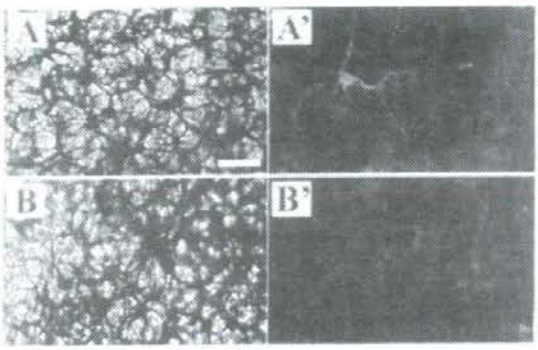

FIG. 7. Expression of huKO in subcutaneous fat tissue of a growing transgenic-cloned pig (O18-3). Bright-field (**A**,**B**) and fluorescence (**A'**,**B'**) microscopic image of subcutaneous fat tissue collected at 7 (**A**,**A'**) and 17 (**B**,**B'**) months after birth. Scale bar = 200 μm.

not shown) of the transduced cells maintained a normal karyotype.

The successful development of the transgenic-cloned pigs accompanying systemic transgene expression is attributable to the high transduction efficiency of our retroviral vector in fetal fibroblasts, as large numbers of provirus were shown by Southern blot analysis to have been introduced into the genomes. The introduction of multiple proviruses into the host genome is a characteristic of retroviral vectors (Hamanaka et al., 2007).

Production of transgenic large animals expressing fluorescent protein genes after transduction using viral vectors has been reported by a number of research groups (Cabot et al., 2001; Chan et al., 2001; Hofmann et al., 2004). In using these animals for research, it is important to consider the types of tissues or cells in which the transduced gene is expressed. Among the huKO pigs produced in the present study, systemic expression of the transduced gene was confirmed in all the pigs examined. Peripheral blood cells except for RBC collected from one 4-month-old transgenic-cloned pig also maintained the expression of huKO gene. It was also confirmed that fluorescence expression level of subcutaneous fat tissue was maintained by at least 17 months after birth. These data indicate stable transgene expression in a growing transgenic pig produced in this study.

Expression of EGFP transduced into embryonic stem cells with a mouse stem cell virus-based vector has been reported to diminish in the resultant chimeric mice (Cherry et al., 2000). In contrast, by using the retroviral vector GCDNsap (Nabekura et al., 2006), we demonstrated high and continued expression of the transgene in immature cells, such as hematopoietic stem cells (Nabekura et al., 2006), neural stem cells (Suzuki et al., 2002a), and hepatic stem cells (Suzuki et al., 2002b). This vector has the dl587rev-derived primer binding site and PCMV-derived LTR in which a 71-bp fragment containing the NCR, a binding site for the transcriptional repressor YY1(Wahlers et al., 2002), was removed by digestion with restriction enzymes and a cloning method (Hamanaka et al., 2007). However, recent studies have shown that the fragment removed by this method also contains a binding site for nuclear factor of activated T cells (NFAT), which is important for maintaining the transcription level of the provirus (Wahlers et al., 2002; Wang et al., 2003). Therefore, in the construction of DΔNsap, the site for YY1 was abolished by site-directed

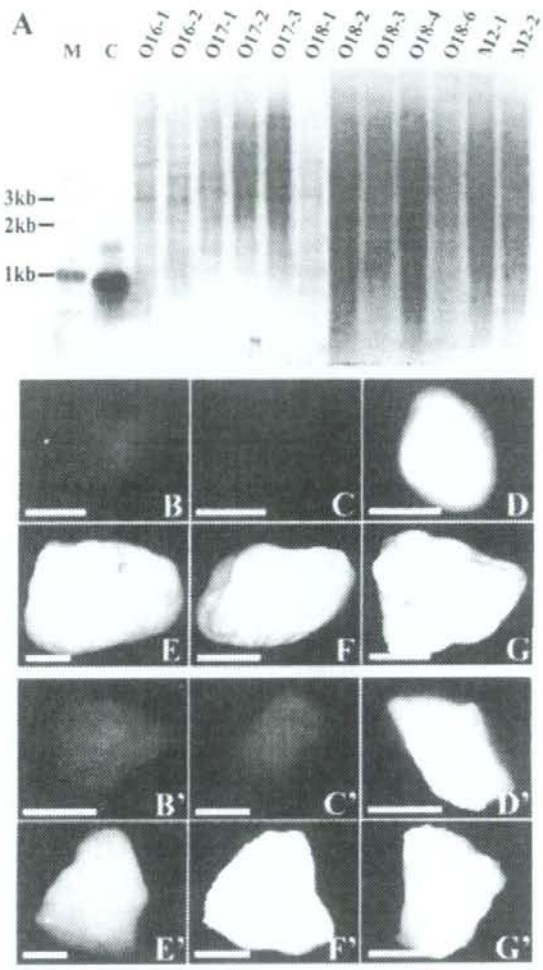

FIG. 8. Multiple provirus integration in the huKO transgenic-cloned pigs and correlation with huKO expression level. (**A**) Southern blot analysis of high molecular-weight DNA isolated from tissues of 12 offspring revealed that 2 to 17 copies of provirus were integrated into the genome of each huKO transgenic-cloned pig (lane O16-1 to lane M2-2). The molecular size marker (lane M) is 1 Kb PLUS DNA Ladder (Invitrogen). Nonlabeled probe DNA was used as a positive control (lane C). Pancreas (**B**–**G**) and skeletal muscle (**B'**–**G'**) tissue of the transgenic pigs showing a lower (pancreas: **B**,**C**, muscle: **B'**,**C'**) and higher (pancreas: **D**–**G**, muscle: **D'**–**G'**) level of huKO expression. Pictures **B**, **B'** and **C**, **C'**, respectively, correspond to O16-1 (two copies) and O18-1 (six copies), which had lower numbers of provirus integrated. Pictures **D** and **D'**, **E** and **E'**, **F** and **F'**, and **G** and **G'**, respectively, correspond to animals O16-2 (11 copies), O17-2 (10 copies), M2-1 (11–13 copies), and M2-2 (11 copies), with higher copy numbers of the integrated provirus. Scale bar = 2.5 mm (**B**,**B'**,**D**,**D'**), 5 mm (**C**,**C'**,**E**–**G**,**E'**–**G'**).

mutagenesis using PCR, while the NFAT binding site remained in the vector (Fig. 1A).

Expression was confirmed in neuronal progenitors in the huKO transgenic-cloned pigs produced in the present study. In addition, expression was also confirmed in cells such as salivary gland progenitor cells (Matsumoto et al., 2007) and pancreatic progenitor cells (data not shown). Together these suggest that the DΔNsap packaged in the VSV-G envelope maintained expression of the transgene in some types of immature cells. Further research is necessary to investigate huKO expression in various tissue stem cells and immature cells in huKO transgenic-cloned pigs.

It should be noted that the huKO cDNA was used as a fluorescent marker in the present study. Fluorescent proteins with excitation/emission spectra in the red or far-red wavelengths such as DsRed have attractive features such as low background autofluorescence (Miyawaki, 2002; Vintersten et al., 2004). In particular, there was little background autofluorescence in the liver and lung of huKO transgenic-cloned pigs, despite the fact that these organs are well known for strong autofluorescence in EGFP transgenic animals (Miyawaki, 2002; Vintersten et al., 2004).

One of the concerns with using a gene of a new fluorescent marker protein to produce transgenic pigs is toxicity of the gene product. DsRed is reported to show toxicity to cells as the result of the obligate tetramer aggregation in the perinulcear/Golgi region (Hadjantonakis et al., 2002). In contrast, huKO, which was cloned from *Fungia concinna* and humanized in the amino acid usage, dimerizes to fluoresce (Karasawa et al., 2004), being attractive feature as a fluorescent marker without apparent cytotoxicity for embryonic and/or fetal development in pigs. However, the long-term effects of huKO expression in the transgenic pigs are yet to be determined. Reproduction testing of a fully matured animal (O18-3; 17-month-old) is currently underway.

Pigs carrying fluorescent protein genes have been produced by various methods, including sperm-mediated gene transfer (Kurome et al., 2006; Webster et al., 2005; Yong et al., 2006), retroviral or lentiviral transduction of oocytes (Cabot et al., 2001), and embryos (Hofmann et al., 2003; Whitelaw et al., 2004), and SCNT using transfected donor cells (Hyun et al., 2003; Lai et al., 2002; Park et al., 2002; Watanabe et al., 2005). The SCNT approach described here allows the concurrent production of transgenic animals expressing a marker gene and nontransgenic clone-siblings from the same donor cells, which provides a useful animal model with donors and recipients of syngenic background. The importance of "translational research" including *in vivo* animal studies has been highly recognized to facilitate clinical applications of new findings in the basic sciences. The huKO transgenic-cloned pigs produced herein may have potential value as large animal models that are essential to translational research.

The present results indicate that the huKO gene can be efficiently transduced into pig fetal fibroblasts using the retroviral vector DΔNsap, and that the nuclear transfer of these cells enables efficient production of transgenic-cloned pigs that systemically express red fluorescence.

Acknowledgments

The authors would like to acknowledge Dr. Eiji Kobayashi and Dr. Yukio Kato for helpful discussion in preparation of the manuscript. The technical expertise of Mr. Yukio Miyata is gratefully acknowledged. This work was supported by the Program for Promotion of Basic Research Activities for Innovative Biosciences (PROBRAIN).

Author Disclosure Statement

The authors declare that no competing financial interests exist.

References

Cabot, R.A., Kühholzer, B., Chan, A.W., et al. (2001). Transgenic pigs produced using in vitro matured oocytes infected with a retroviral vector. Anim. Biotechnol. 12, 205–214.

Chan, A.W., Chong, K.Y., Martinovich, C., et al. (2001). Transgenic monkeys produced by retroviral gene transfer into mature oocytes. Science 291, 309–312.

Cherry, S.R., Biniszkiewicz, D., van Parijs, L., et al. (2000). Retroviral expression in embryonic stem cells and hematopoietic stem cells. Mol. Cell Biol. 20, 7419–7426.

Forsberg, E.J., Strelchenko, N.S., Augenstein, M.L., et al. (2002). Production of cloned cattle from in vitro systems. Biol. Reprod. 67, 327–333.

Freshney, R.I. (2005). Primary culture. In *Culture of Animal Cells* (Wiley-Liss, Hoboken, NJ), pp. 175–198.

Fujimura, T., Murakami, H., Kurome, M., et al. (2008). Effects of recloning on the efficiency of production of 1,3-galactosyltransferase-knockout pigs. J. Reprod. Dev. 54, 58–62.

Funahashi, H., and Day, B.N. (1993). Effects of the duration of exposure to hormone supplements on cytoplasmic maturation of pig oocytes in vitro. J. Reprod. Fertil. 98, 179–185.

Hadjantonakis, A.K., and Nagy, A. (2001). The color of mice: in the light of GFP-variant reporters. Histochem. Cell Biol. 115, 49–58.

Hadjantonakis, A.K., Macmaster, S., and Nagy, A. (2002). Embryonic stem cells and mice expressing different GFP variants for multiple non-invasive reporter usage within a single animal. BMC Biotechnol. 2, 11.

Hamanaka, S., Nabekura, T., Otsu, M., et al. (2007). Stable transgene expression in mice generated from retrovirally transduced embryonic stem cells. Mol. Ther. 15, 560–565.

Hayakawa, H., Hayashita-Kinoh, H., Nihira, T., et al. (2007). The isolation of neural stem cells from the olfactory bulb of Parkinson's disease model. Neurosci. Res. 57, 393–398.

Hofmann, A., Kessler, B., Ewerling, S., et al. (2003). Efficient transgenesis in farm animals by lentiviral vectors. EMBO Rep. 4, 1054–1060.

Hofmann, A., Zakhartchenko, V., Weppert, M., et al. (2004). Generation of transgenic cattle by lentiviral gene transfer into oocytes. Biol. Reprod. 71, 405–409.

Hyun, S., Lee, G., Kim, D., et al. (2003). Production of nuclear transfer-derived piglets using porcine fetal fibroblasts transfected with the enhanced green fluorescent protein. Biol. Reprod. 69, 1060–1068.

Iguma, L.T., Lisauskas, S.F., Melo, E.O., et al. (2005). Development of bovine embryos reconstructed by nuclear transfer of transfected and non-transfected adult fibroblast cells. Genet. Mol. Res. 4, 55–66.

Karasawa, S., Araki, T., Nagai, T., et al. (2004). Cyan-emitting and orange-emitting fluorescent proteins as a donor/acceptor pair for fluorescence resonance energy transfer. Biochem. J. 381, 307–312.

Kurome, M., Fujimura, T., Murakami, H., et al. (2003). Comparison of electro-fusion and intracytoplasmic nuclear injection methods in pig cloning. Cloning Stem Cells 5, 367–378.

Kurome, M., Ueda, H., Tomii, R., et al. (2006). Production of transgenic-clone pigs by the combination of ICSI-mediated gene transfer with somatic cell nuclear transfer. Transgenic Res. 15, 229–240.

Lai, L., Park, K.W., Cheong, H.T., et al. (2002). Transgenic pig expressing the enhanced green fluorescent protein produced by nuclear transfer using colchicine-treated fibroblasts as donor cells. Mol. Reprod. Dev. 62, 300–306.

Long, J.Z., Lackan, C.S., and Hadjantonakis, A.K. (2005). Genetic and spectrally distinct in vivo imaging: embryonic stem cells and mice with widespread expression of a monomeric red fluorescent protein. BMC Biotechnol. 5, 20.

Luche, H., Webwe, O., Rao, T.N., et al. (2007). Faithful activation of an extra-bright red fluorescent protein in "knock-in" Cre-reporter mice ideally suited for lineage tracing studies. Eur. J. Immunol. 37, 43–53.

Lunney, J.K. (2007). Advances in swine biomedical model genomics. Int. J. Biol. Sci. 3, 179–184.

Matsumoto, S., Okumura, K., Ogata, A., et al. (2007). Isolation of tissue progenitor cells from duct-ligated salivary glands of swine. Cloning Stem Cells 9, 176–190.

Miyawaki, A. (2002). Green fluorescent protein-like proteins in reef Anthozoa animals. Cell Struct. Funct. 27, 343–347.

Murakami, T., and Kobayashi, E. (2005). Color-engineered rats and luminescent LacZ imaging: a new platform to visualize biological processes. J. Biomed. Opt. 10, 41204.

Nabekura, T., Otsu, M., Nagasawa, T., et al. (2006). Potent vaccine therapy with dendritic cells genetically modified by the gene-silencing-resistant retroviral vector GCDNsap. Mol. Ther. 13, 301–309.

Nagashima, H., Hiruma, K., Saito, H., et al. (2007). Production of live piglets following cryopreservation of embryos derived from in vitro-matured oocytes. Biol. Reprod. 76, 900–905.

Naruse, K., Ishikawa, H., Kawano, H., et al. (2005). Production of a transgenic pig expressing human albumin and enhanced green fluorescent protein. J. Reprod. Dev. 51, 539–546.

Okabe, M., Ikawa, M., Kominami, K., et al. (1997). "Green mice" as a source of ubiquitous green cells. FEBS Lett. 407, 313–319.

Park, K.W., Lai, L., Cheong, H.T., et al. (2002). Mosaic gene expression in nuclear transfer-derived embryos and the production of cloned transgenic pigs from ear-derived fibroblasts. Biol. Reprod. 66, 1001–1005.

Petters, R.M. (1994). Transgenic livestock as genetic models of human disease. Reprod. Fertil. Dev. 6, 643–645.

Petters, R.M., and Wells, K.D. (1993). Culture of pig embryos. J. Reprod. Fertil. Suppl. 48, 61–73.

Petters, R.M., Alexander, C.A., Wells, K.D., et al. (1997). Genetically engineered large animal model for studying cone photoreceptor survival and degeneration in retinitis pigmentosa. Nat. Biotechnol. 15, 965–970.

Prather, R.S., Hawley, R.J., Carter, D.B., et al. (2003). Transgenic swine for biomedicine and agriculture. Theriogenology 59, 115–123.

Rogers, C.S., Hao, Y., Rokhlina, T., et al. (2008). Production of CFTR-null and CFTR-DeltaF508 heterozygous pigs by adeno-associated virus-mediated gene targeting and somatic cell nuclear transfer. J. Clin. Invest. 118, 1571–1577.

Sato, Y., Igarashi, Y., Hakamata, Y., et al. (2003). Establishment of Alb-DsRed2 transgenic rat for liver regeneration research. Biochem. Biophys. Res. Commun. 311, 478–481.

Suzuki, A., Obi, K., Urabe, T., et al. (2002a). Feasibility of ex vivo gene therapy for neurological disorders using the new retroviral vector GCDNsap packaged in the vesicular stomatitis virus G protein. J. Neurochem. 82, 953–960.

Suzuki, A., Zheng, Y.W., Kaneko, S., et al. (2002b). Clonal identification and characterization of self-renewing pluripotent stem cells in the developing liver. J. Cell. Biol. 156, 173–184.

Tomii, R., Kurome, M., Ochiai, T., et al. (2005). Production of cloned pigs by nuclear transfer of preadipocytes established from adult mature adipocytes. Cloning Stem Cells 7, 279–288.

Vintersten, K., Monetti, C., Gertsenstein, M., et al. (2004). Mouse in red: red fluorescent protein expression in mouse ES cells, embryos, and adult animals. Genesis 40, 241–246.

Wahlers, A., Kustikova, O., Zipfel, P.F., et al. (2002). Upstream conserved sequences of mouse leukemia viruses are important for high transgene expression in lymphoid and hematopoietic cells. Mol. Ther. 6, 313–320.

Walker, S.C., Shin, T., Zaunbrecher, M.Z., et al. (2002). A highly efficient method for porcine cloning by nuclear transfer using in vitro-matured oocytes. Cloning Stem Cells 4, 105–111.

Wang, L., Haas, D., Halene, S., et al. (2003). Effects of the negative control region on expression from retroviral LTR. Mol. Ther. 7, 438–440.

Watanabe, S., Iwamoto, M., Suzuki, S., et al. (2005). A novel method for the production of transgenic cloned pigs: electroporation-mediated gene transfer to non-cultured cells and subsequent selection with puromycin. Biol. Reprod. 72, 309–315.

Webster, N.L., Forni, M., Bacci, M.L., et al. (2005). Multi-transgenic pigs expressing three fluorescent proteins produced with high efficiency by sperm mediated gene transfer. Mol. Reprod. Dev. 72, 68–76.

Whitelaw, C.B., Radcliffe, P.A., Ritchie, W.A., et al. (2004). Efficient generation of transgenic pigs using equine infectious anaemia virus (EIAV) derived vector. FEBS Lett. 571, 233–236.

Yamada, M., Onodera, M., Mizuno, Y., et al. (2004). Neurogenesis in olfactory bulb identified by retroviral labeling in normal and 1-methyl-4-phenyl-1,2,3,6-tetrahydropyridine-treated adult mice. Neuroscience 124, 173–181.

Yin, X.J., Tani, T., Yonemura, I., et al. (2002). Production of cloned pigs from adult somatic cells by chemically assisted removal of maternal chromosomes. Biol. Reprod. 67, 442–446.

Yin, X.J., Lee, H.S., Yu, X.F., et al. (2007). Generation of cloned transgenic cats expressing red fluorescence protein. Biol. Reprod. 78, 425–431.

Yong, H.Y., Hao, Y., Lai, L., et al. (2006). Production of a transgenic piglet by a sperm injection technique in which no chemical or physical treatments were used for oocytes or sperm. Mol. Reprod. Dev. 73, 595–599.

Zakhartchenko, V., Mueller, S., Alberio, R., et al. (2001). Nuclear transfer in cattle with non-transfected and transfected fetal or cloned transgenic fetal and postnatal fibroblasts. Mol. Reprod. Dev. 60, 362–369.

Address reprint requests to:
Hiroshi Nagashima, Ph.D.
Laboratory of Developmental Engineering
Department of Life Science, School of Agriculture
Meiji University
1-1-1 Higashimita, Tama, Kawasaki 214-8571, Japan

E-mail: hnagas@isc.meiji.ac.jp

THE JOURNAL OF GENE MEDICINE
J Gene Med 2008; 10: 965–971.
Published online 9 July 2008 in Wiley InterScience (www.interscience.wiley.com) DOI: 10.1002/jgm.1232

RESEARCH ARTICLE

A new red fluorescent protein that allows efficient marking of murine hematopoietic stem cells

Seiko Sanuki[1]
Sanae Hamanaka[1]
Shin Kaneko[1]
Makoto Otsu[2]
Satoshi Karasawa[3]
Atsushi Miyawaki[3]
Hiromitsu Nakauchi[2]
Toshiro Nagasawa[1]
Masafumi Onodera[1]*

[1]*Advanced Biomedical Applications, Graduate School of Comprehensive Human Sciences, University of Tsukuba, Tsukuba, Ibaraki, Japan*

[2]*Laboratory of Stem Cell Therapy, Center for Experimental Medicine, Institute of Medical Science, the University of Tokyo, Minatoku, Tokyo, Japan*

[3]*Laboratory for Cell Function and Dynamics, Advanced Technology Development Group, Brain Science Institute (RIKEN), Wako, Saitama, Japan*

*Correspondence to:
Masafumi Onodera, Laboratory of Genetic Diagnosis and Gene Therapy, Department of Genetics, National Research Institute for Child Health and Development, 2-10-1 Okura, Setagaya-ku, Tokyo 157-8535, Japan.
E-mail: monodera@nch.go.jp

Received: 20 December 2007
Revised: 1 May 2008
Accepted: 30 May 2008

Abstract

Background Genetic marking of hematopoietic stem cells (HSCs) with multiple fluorescent proteins (FPs) would allow analysis of their features, including interaction with adjacent cells. However, there are few red FPs that are comparable to green FPs in terms of low toxicity and high fluorescent intensity. This study has evaluated the usefulness of Kusabira Orange (KO) originated from the coral stone *Fungia concinna* as a red FP for marking of HSCs

Methods A vector used was the MSCV-type retroviral vector, DΔNsap that has the PCC4 cell-passaged myeloproliferative sarcoma virus derived long terminal repeat devoid of a binding site for YY1 and the primer-binding site derived from the dl587rev, respectively. The vector was cloned with the codon-optimized KO cDNA for higher expression in mammalian cells (huKO) and converted to the corresponding retroviruses pseudotyped with the vesicular stomatitis virus G envelope protein, then transduced into c-KIT$^+$Sca-1$^+$Lineage$^-$ cells obtained from C57BL/6 (Ly5.1) mice followed by transplantation into lethally irradiated Ly5.2 mice.

Results Approximately 70% of donor-derived cells highly expressed huKO at 16 weeks post-transplantation. Furthermore, the high expression of huKO was also detected in serially transplanted mice, suggesting that expression of huKO *per se* had little deleterious effect on murine hematopoiesis. In double marking experiments, huKO-expressing hematopoietic cells were easily distinguished from those expressing EGFP by flow cytometery and fluorescent microscope analysis.

Conclusions Overall, the results obtained from the present study suggest that huKO can be used as a valuable and versatile red fluorescent marker for HSCs. Copyright © 2008 John Wiley & Sons, Ltd.

Keywords gene transfer; hematopoietic stem cells; red fluorescent protein; retroviral vectors; VSV-G

Introduction

Hematopoietic stem cells (HSCs) are defined as cells with unique features of self-renewal and differentiation into all lineages of hematopoietic cells [1]. The processes of their proliferation, differentiation, and hibernation are tightly controlled by both intrinsic and extrinsic factors, such as intra-cellular signal mechanisms exerted by multiple gene functions and interactions with adjacent cells, respectively [2–5]. Although a number of sophisticated studies with advanced molecular technologies have revealed an outline of the mechanisms underlying these processes, there is still much to be determined. One

effective way to help these studies involves the expression of gene of interest or its mutant form into the HSCs using retroviral vectors along with a fluorescent marking protein (FP) cDNA, which should allow identification of the cellular location of the molecules under investigation and/or the position of HSCs temporally and spatially within living cells and organisms [6]. Although a considerable number of FPs with unique and distinct spectral properties have been identified and used for following genes or marking cells, variants of green FPs originated from the jellyfish *Aequorea victoria*, especially its optimized form, enhanced green fluorescent protein (EGFP) is the most widely used for HSCs because of lower toxicity and higher fluorescent intensity [7,8].

Given that EGFP is the first choice for a green FP in marking experiments of HSCs, red FPs whose emission is completely distinguishable from that of EGFP with flow cytometery or fluorescent microscope would facilitate to analyse interactions between genes or cells. Although *Discosoma* sp. red fluorescent protein (DsRed) that was cloned from the reed coral *Discosoma* sp. is mostly used for such purposes [9,10], it is unlikely to properly mark HSCs due to high toxicity resulting from cytoplasmic aggregates of the tetramized protein [11]. With the aim of reducing toxicity, mutant forms or DsRed that fluoresce in the monomeric or tandem dimeric form have been developed [12–15]. Kusabira Orange (KO), which has been recently cloned from the coral stone *Fungia concinna* (Kusabira Ishi in Japanese), also has red fluorescence properties in a dimeric form [16]. In the present study, we evaluated the usefulness of codon-optimized KO (huKO) for higher expression in mammalian cells as a suitable red tracer for HSCs in serial transplantation experiments.

Materials and methods

Mice

C57BL/6 (B6-Ly5.1) mice were purchased from Nihon Clea (Tokyo, Japan); congenic mice (B6-Ly5.2) were bred and maintained at the University of Tsukuba Animal Research Center. An experimental design of the present study was approved by the Animal Experimental Committee of the University of Tsukuba.

huKO retroviral vector and transduction into mouse HSCs

The retroviral vector DΔNsap was constructed by abolishing the YY1 binding site in the PCC4 cell-passaged myeloproliferative sarcoma virus (PCMV) derived long terminal repeat (LTR) of GCDsap [17] by site-directed mutagenesis using the polymerase chain reaction (PCR) technique (Figure 1A). *NcoI-NotI* fragments of huKO cDNA digested from phKO1-MC1 (AM-V0045; MBL, Tokyo, Japan) were inserted into the *NcoI-NotI* digested

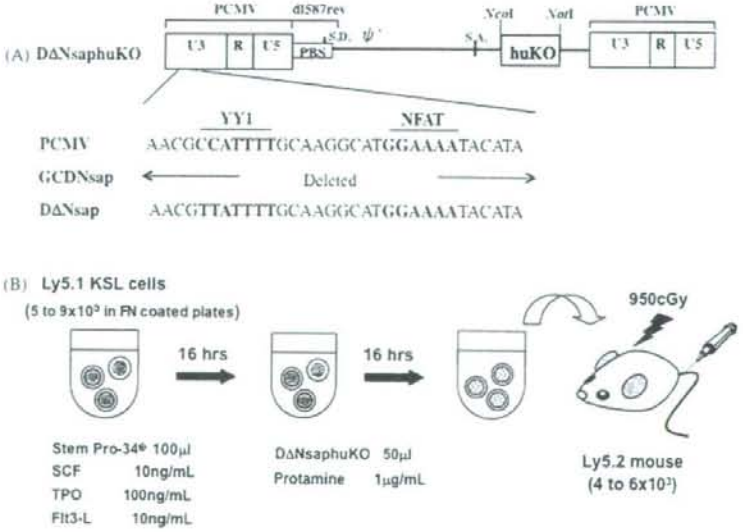

Figure 1. Structure of the retroviral vector DΔNsaphuKO (A). DΔNsap has the PCMV derived LTR in which the binding site for YY1 (CCATTTT) was abolished by the site-directed mutagenesis by PCR, whereas the NFAT binding site is still functional. By contrast, GCDNsap has the PCMV derived LTR that lacks both binding sites for YY1 and NFAT. The *NcoI-NotI* fragments containing huKO cDNA were cloned into the corresponding site of the vector. A dot box presents the primer binding site derived from the dl587rev. PCMV, PCC4-cell passaged myeloproliferative sarcoma virus; Ψ^+, packaging signal. Five to nine thousand cells of c-KIT +/Sca1 +/Lineage− (KSL) cells obtained from Ly5.1 mouse bone marrow were cultured in 100 μl of serum-free medium (Stem Pro-34) containing SCF, thrombopoietin (TPO), and Flt3-ligand (Flt3-L) using a fibronectin (FN)-coated well of 96-well plates for 16 h and transduced with the huKO cDNA by adding 50 μl of the virus together with protamine sulfate into the culture, and were then used for subsequent experiments 16 h later

DOI: 10.1002/jgm

vector to generate DΔNhuKO. The vector was converted to the corresponding retroviruses that were pseudotyped with the vesicular stomatitis virus G protein (VSV-G) envelope protein by transduction into 293gpg cells [18]. EGFP-expressing retrovirus (DΔNEGFP) was also produced following the same procedure above. The titers of both recombinant retroviruses were approximately 1.0×10^7 infectious units/ml as assessed on Jurkat cells.

c-KIT$^+$Sca1$^+$Lineage$^-$ cells (KSL cells) were purified from bone marrow of 6–8-week-old Ly5.1 mice by dual-laser FACS Vantage (Becton-Dickinson, Franklin Lakes, NJ, USA) as described previously [19]. Sorted KSL cells ($5–9 \times 10^3$) were cultured in 100 μl of StemPro-34 SFM (Gibco BRL, Rockville, MD, USA) containing mouse stem cell factor (10 ng/ml; Kirin Brewery Co., Takasaki, Japan), human thrombopoietin (100 ng/ml; Peprotech, Rocky Hill, NJ, USA), and mouse Flt3-ligand (10 ng/ml, Kirin Brewery Co.) for 16 h on CH293 recombinant fibronectin (RetroNectin, Takara Bio, Otsu, Japan) coated 96-well plates. Fifty microliters of the virus supernatants with 5 μg/ml protamine sulfate (Sigma Aldrich, St Louis, MO, USA) was then added to the culture (multiplicity of infection = 100). After 16 h, $4–6 \times 10^3$ transduced cells were transplanted intravenously into 950 cGy irradiated Ly5.2 mice and the chimerism and huKO expression of donor cells in transplanted mice were determined with FACS Calibur (Becton-Dickinson) at different time points. In serial transplantation experiments, 1×10^5 bone marrow cells obtained from the primary or secondary recipients at 12 weeks post-transplantation were transplanted to lethally irradiated secondary or tertiary mice.

Cell surface analysis

Mononuclear cells were isolated from peripheral blood or bone marrow of the recipient mice and stained with a biotinylated anti-Ly5.1 antibody, followed by straptavidin-allophycocyanin (APC). Cells were also stained with antibodies against lineage markers; fluorescein isothiocyanate (FITC) or Cy5-conjugated antibodies for Gr-1, Mac-1, B220, CD4, and CD8. All antibodies were purchased from BD Pharmingen (San Diego, CA, USA). Multicolor analyses were performed with FACS Calibur. Expression of huKO was detected by the FL2 channel (585 ± 21 nm) of FACS Calibur.

Colony assay

Two hundred KSL cells transduced with huKO or EGFP cDNA were cultured in 1 ml of methylcellulose medium containing mouse stem cell factor (SCF), mouse interleukin (IL)-3, human IL6, and human erythropoietin (M3232; Stem Cell Technology, Vancouver, Canada) in a 3.5-mm dish for 14 days. huKO- or EGFP-expressing colonies consisting of more than 50 cells were counted by fluorescence microscopy (Axiovert135, Carl Zeiss, Jena, Germany; 450–490/LP520 for GFP and 546/LP590 for huKO).

Results

Generation of retroviruses expressing huKO

We have demonstrated high and continued expression of the transgene in immature cells such as HSCs, neural stem cells, and hepatic stem cells by using the gene silencing resistant retroviral vectors GCDNsap [18,20,21]. The vector has the dl587rev-derived primer binding site and PCMV-derived LTR in which 71-bp fragments containing the negative control region, a binding site for the transcriptional repressor YY1, were removed by digestion of restriction enzymes and ligation [18]. However, recent studies have demonstrated the removed fragments also contain a binding site for the nuclear factor of activated T cells (NFAT) family, resulting in lowering the viral transcription [22,23]. Therefore, the site for YY1 in DΔNsap was abolished by site-directed mutagenesis using the PCR technique whereas the site for NFAT remained in the vector (Figure 1A). The vector encoding the huKO cDNA was converted into the corresponding retroviruses in 293gpg cells that were engineered to express VSV-G under the tetracycline-induced system (tet-off system). The virus titer was approximately 1.0×10^7 infectious units as assessed on Jurkat cells. No replication competent retrovirus was detected.

Transduction of the huKO cDNA into murine HSCs

Because the population of HSCs is very tiny and most HSCs remain at the quiescent stage, they are generally stimulated with cytokines for a few days to undergo mitotic cell division for retrovirus infection. However, such cytokine-induced stimulation often leads to HSCs differentiating into less immature cells that have, if any, little capability of bone marrow reconstitution. In addition, serum present in the culture also induces differentiation of HSCs. To preserve the immaturity at the same times as inducing their cell division [24], KSL cells obtained from Ly5.1 mice were pre-stimulated in serum-free medium containing the minimal, but essential cytokines such as SCF, Flt3-ligand, and thrombopoietin for 16 h, exposed to the concentrated serum-free virus supernatants in the culture for 16 h, and then used for subsequent experiments (Figure 1B).

With the transduction protocol, approximately 70% of treated cells expressed huKO and such high transduction efficiency was also confirmed by colony forming cell assays. Importantly, huKO expression was clearly distinguishable from that of EGFP under fluorescence microscope observation (Figure 2A) and by FACS Calibur (Figure 2B) when the cells were mixed with those expressing EGFP.

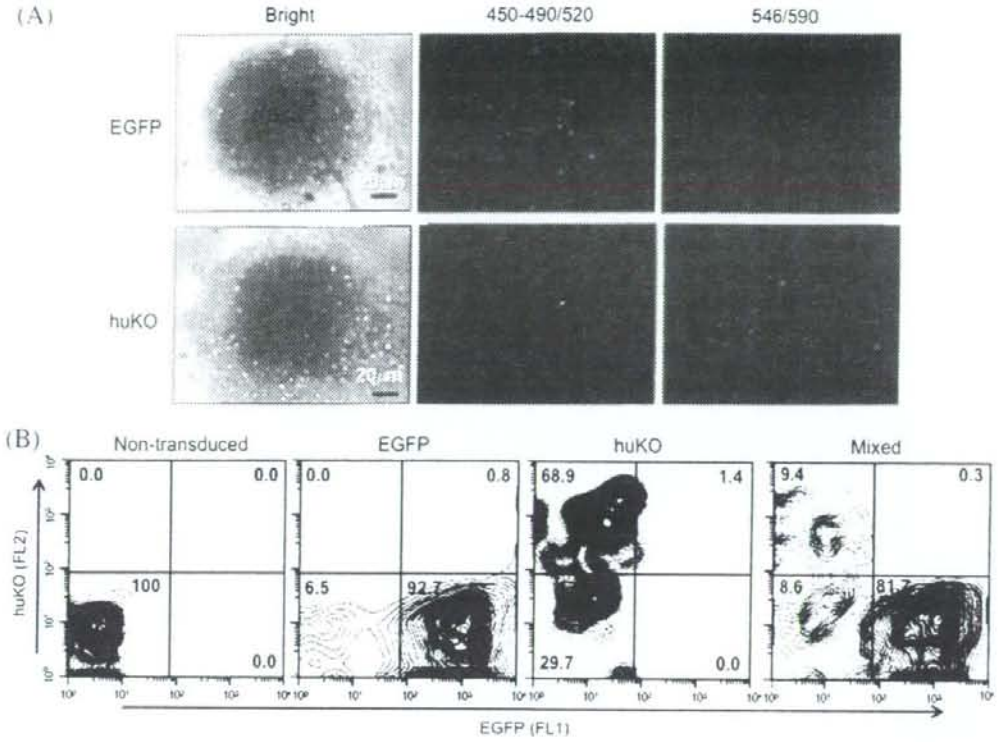

Figure 2. Two hundred KSL cells transduced with the huKO or EGFP cDNA were cultured in 1 ml of methycellulose medium containing mSCF, mIL3, hIL6 and human erythropoietin for 14 days. Representative colonies of cells transduced with the EGFP (upper panels) or huKO cDNA (lower panels) are shown (A). Colonies consisting of more than 50 cells were observed by fluorescent microscopy (Axiovert135; Carl Zeiss). Excitation and emission filters for EGFP or huKO were 450–490/LP520 and 546/LP590, respectively. Cells collected from each colony were analysed individually or after one-to-one mixture by FACS Calibur (B). Nontransduced cells were used as a reference

Reconstitution of bone marrow hematopoiesis by HSCs expressing huKO

Transduced KSL cells derived from Ly5.1 mice were transplanted into lethally irradiated Ly5.2 mice intravenously at 4–6 × 10^3 cells per mouse and the expression of huKO in the peripheral blood of transplanted mice was analysed at every 3 weeks post-transplantation by flow cytometery. Among Ly5.1 positive cells that occupied 40–70% of peripheral leukocytes in the transplanted mice, more than 70% expressed huKO with high fluorescent intensity and such expression was maintained over 16 weeks post-transplantation (Figure 3A). huKO expression was detected in each hematopoietic lineage, such as the B cell, T cell, or myeloid lineages, in the peripheral blood, thymus, and bone marrow (data not shown). To assess long-term expression of huKO by HSCs, bone marrow cells of transplanted mice were serially transplanted into Ly5.2 mice at 12 weeks post-transplantation. Expression of huKO was still observed in more than 80% of Ly5.1 positive cells in secondarily and tertiarily transplanted mice (Figure 3B).

Co-expression of huKO with EGFP by HSCs

Having identified that huKO is a proper red FP for hematopoietic cells, we next assessed whether it could be distinguished from EGFP by flow cytometery without any extra-filters. Isolated Ly5.1 KSL cells were double-infected with retroviruses expressing either huKO or EGFP by adding the supernatants into the same culture and transplanted into Ly5.2 recipient mice. Although the percentages of EGFP- and huKO-expressing cells varied among mice because of different transduction efficiency in each experiment, the populations of cells expressing either huKO or EGFP or both in peripheral blood (Figure 4A) and thymus (Figure 4B) were classified by flow cytometery during the observation time up to 16 weeks. The cell populations with different intensity of huKO expression were observed in the peripheral blood, thymus, and bone marrow in some of the mice, suggesting that multiple HSCs were infected with retroviruses expressing huKO and some with a different intensity of huKO expression reconstituted bone marrow hematopoiesis, independently. To assess whether huKO expression was less toxic to bone marrow compared to

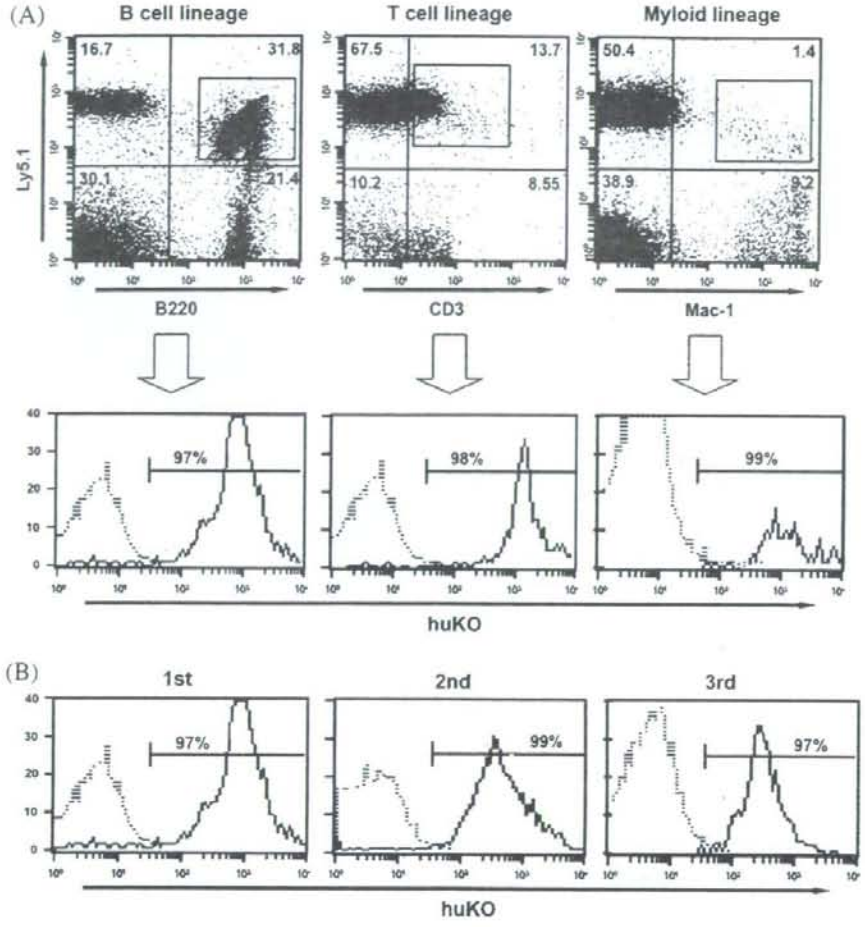

Figure 3. Four to six thousand huKO transduced Ly5.1 mouse cells were transplanted into lethally irradiated Ly5.2 mice intravenously and huKO expression in peripheral blood of transplanted mice was analysed at 16 weeks post-transplantation (A). Peripheral blood cells obtained from transplanted mice were stained with anti-Ly5.1 antibody (APC) and FITC-conjugated lineage markers (upper panels). Cells positive for Ly5.1 and each lineage marker (framed by open square) were analysed by FACS Calibur to determine the huKO expression in each lineage derived from donor cells (lower panels). huKO expression was also analysed in the peripheral blood of serially transplanted mice (B). Bone marrow cells (1×10^5) obtained from mice at 12 weeks post-transplantation were transplanted into secondarily or tertiarily lethally irradiated mice. Results shown are representative FACS analyses of peripheral blood in mice at 12 weeks post-transplantation. A dotted line inidicates huKO expression levels of Ly5.2 cells of each lineage from the recipient mice

EGFP, the chimerism of donor cells and percentages of the huKO expressing cells of primarily and secondarily transplanted mice were analysed at 3, 9, and 16 weeks post-transplantation (Figure 5). Both parameters, such as chimerism and the percentage of FP expressing cells, were hardly distinguishable between mice transplanted with EGFP- or huKO-expressing cells, suggesting that huKO were similar to EGFP with respect to marking hematopoietic cells.

Discussion

We have demonstrated the feasibility of huKO as a red fluorescent marker for hematopoietic cells in serial transplantation experiments in which murine HSCs were transduced with the huKO cDNA using the DΔNsap. Transduced cells serially transplanted were capable of reconstituting bone marrow hematopoiesis of lethally irradiated mice. Furthermore, double infection of HSCs together with the retrovirus expressing EGFP allowed multi-color tracing of hematopoietic cells *in vivo*, suggesting that huKO was a proper FP along with EGFP.

The original gene of huKO was cloned from *F. concinna* known as Kusabira-Ishi in Japanese and modified by attaching an artificial amino acid sequence (Met-Ser-Val-Ile-Lys-Pro-Glu) to the N-terminus of the gene in reference to other red FPs [16] and humanizing the amino acid usage of the gene to synthesize the humanized

DOI: 10.1002/jgm

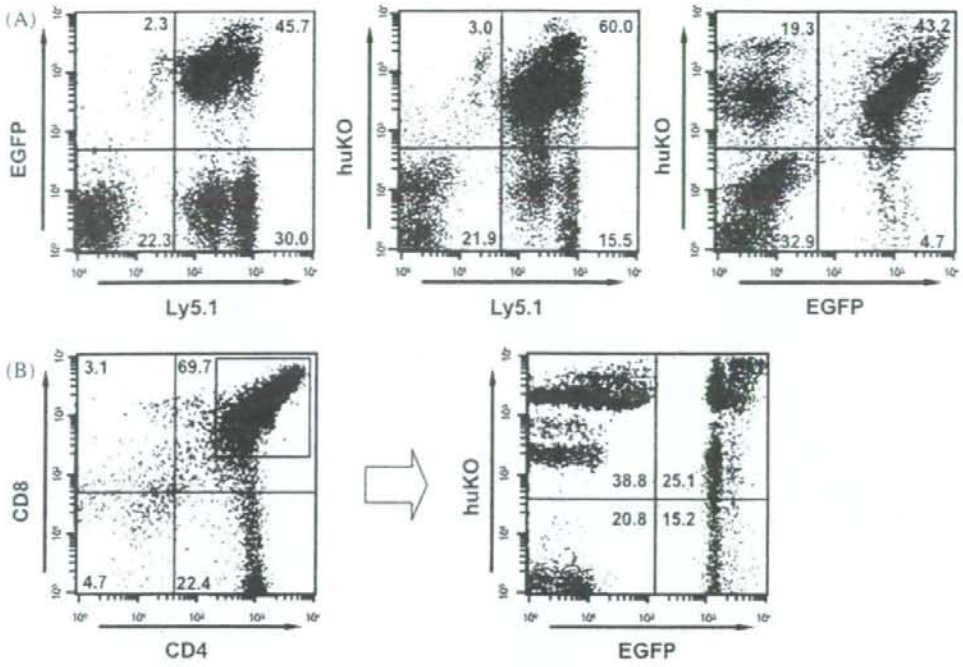

Figure 4. Double transduction of KSL cells with huKO- and EGFP-expressing retroviruses. KSL cells obtained from Ly5.1 mice were transduced with the EGFP and huKO cDNAs and transplanted into lethally irradiated Ly5.1 mice intravenously. Peripheral blood cells of transplanted mice at 16 weeks post-transplantation were stained with anti-Ly5.1 antibody and analysed with FACS Calibur (A). Representative FACS patterns of Ly5.1/EGFP (left), Ly5.1/huKO (middle), and EGFP/huKO (right) are shown. Thymic cells were also obtained from mice at 16 weeks post-transplantation and were stained with CD4 (Cy5) and CD8 (APC) (B, left). Double positive cells for CD4 and CD8 (framed by open square) were analysed in EGFP and huKO expression (B, right)

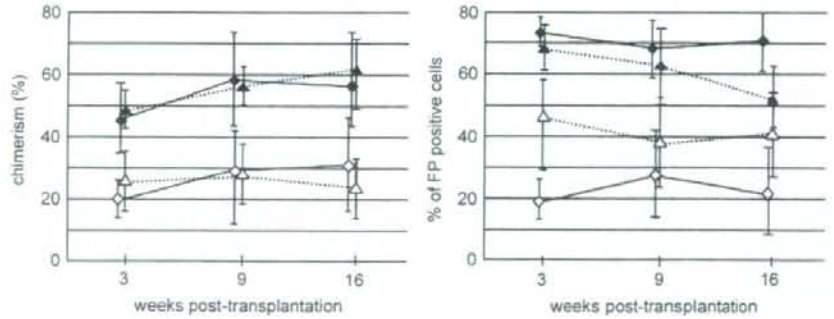

Figure 5. Time course of the chimerism of donor cells (left) and percentages of FP expression (right) in primarily and secondarily transplanted mice. In serial transplantation experiments, peripheral blood cells of mice transplanted with EGFP or huKO-transduced cells were analysed in Ly5.1 and each FP expression at 3, 9, and 16 weeks post-transplantation with FACS Calibur. Chimerism was determined by calculating percentages of Ly5.1 positive cells in total cells. The population of FP positive cells (% of FP positive cells) means percentages of EGFP or huKO-expressing cells in Ly5.1 positive cells. Mice primarily (▲) and secondarily (△) transplanted with EGFP-transduced cells; mice primarily (♦) and secondarily (◊) transplanted with huKO-transduced cells. Data are the mean ± SD from an average of five independent experiments

Kusabira Orange (huKO) cDNA [AM-V0045, MBL, Japan; https://res.mbl.co.jp/catalog/flprotein.html]. huKO displays a major absorption wavelength maximum at 548 nm with a slight shoulder at 515 nm and emitted a bright orange fluorescence, peaking at 561 nm, whereas the excitation/emission maxima of DsRed is 558 and 583 nm, respectively. Analytical equilibrium ultracentrifugation analysis calculated the absolute molecular mass of 77.0 kDa, which was 2.75-fold greater than that (28.0 kDa) deduced from the primary structure of the protein, suggesting that huKO may exist in a heterogeneous oligomeric state, including dimers and tetramers.